Excitation of ^{229m}Th in the electron bridge via continuum, as a scattering process

A. Ya. Dzyublik*

Institute for Nuclear Research, National Academy of Sciences of Ukraine, avenue Nauki 47, 03680 Kyiv, Ukraine and National Research Nuclear University MEPhI, Kashirskoe shosse 31, 115409 Moscow, Russian Federation

(Received 5 May 2020; accepted 17 July 2020; published 5 August 2020)

Excitation of the isomer ^{229m}Th with energy 8.3 eV in the electron bridge (EB) via continuous electron spectrum is treated as a two-step process. At first an outer atomic electron absorbs the laser photon and leaves the atom, afterwards it returns to the atom transferring its energy to the nucleus. This EB transition is described in the framework of strict scattering theory for the atomic-nuclear system with two overlapping resonances. The derived EB cross section differs in some details from the results of P. V. Borisyuk *et al.* [Phys. Rev. C **100**, 044306 (2019)].

DOI: 10.1103/PhysRevC.102.024604

I. INTRODUCTION

The ^{229}Th takes up a unique place in the nuclear chart, having the first-excited isomeric level $3/2^+$ with extremely low energy, which lies in the ultraviolet region. Intense interest in the isomer ^{229m}Th is dictated for many years by its fascinating applications, where the most striking one is the nuclear clock [1–3], which will become a more precise standard of frequency than already existing optical clocks. Besides, it would be highly stable against external influences because of the electron shielding. Among other applications there is a nuclear laser in the optical region [4], search of time variation of the physical constants [5–9], the Mössbauer effect at ^{229}Th nuclei with the absorption and emission spectra represented only by phononless lines [10], etc.

Kroger and Reich [11] have been the first to show that within 100 eV from $5/2^+[633]$ ground state of ^{229}Th lies the level $3/2^+[631]$. It is a band head for the rotational band with the second level $5/2^+[631]$ at 29.2 keV. Further measurements showed that the isomeric level lies in optical region with the energy $E_{\rm is}$ equal to 3.5 eV [12] or 5.5 eV [13]. However, recently it was already reported $E_{\rm is} = 7.8$ eV [14], 8.30 ± 0.92 eV [15]. In these works [11–15] the energy $E_{\rm ion}$ was measured indirectly by comparing the energies of γ transition from the level 29.2 keV to the isomeric one and cross-band transition to the ground state.

Only Wense *et al.* [16] succeeded to determine $E_{\rm is}$ of the isomer ^{229m}Th, measuring directly the energy of conversion electrons, produced in the decay of the isomer. They established that $E_{\rm is}$ lies in the interval from 6.3–18.3 eV. The last refined experiment of Seiferle *et al.* [17] provided a more definite result 8.28 ± 0.17 eV, which can be considered today as the most reliable evidence. Note also that the ^{229m}Th in neutral atom predominantly decays through the internal conversion (IC) channel (the conversion coefficient $\alpha \approx 10^9$ [17]).

All these investigations used α decay of ^{233}U to populate ^{229m}Th via the second-excited level 29.2 keV. Verlinde *et al.* [18] proposed to use for this aim β decay of ^{229}Ar and discussed the advantages of this alternative. Most straightforward optical experiment had been done by Jeet *et al.* [19], who excited ^{229m}Th by synchrotron radiation lying in the ultraviolet region and observed spontaneous decay of the isomer. However strange it may seem, they stated that the energy is outside the interval 7.3–8.8 eV, which contradicts the results of Ref. [17]. Another version of the ^{229}Th population by narrow beam of synchrotron radiation via the second level 29.2 keV has been reported in Ref. [20].

The discovery of such extremely low-lying isomer-stimulated theoretical studies of the possibility of ^{229m}Th excitation by optical lasers [21–27]. Starting from the pioneering works of Tkalya [21,22], different kinds of the electronic bridges have been analyzed, evolving one or two lasers. Recall that the name electron bridge (EB) was suggested by Krutov [28] for the processes of the third and higher order with intermixed nuclear and atomic transitions. Different laser excitation schemes for ^{229m}Th have been considered also in Ref. [29]. The only successful experiment [30] on ^{229m}Th with optical lasers was addressed to study of the hyperfine structure of its spectra. It allowed us to define the magnetic and quadrupole moments, as well as the mean-square radius of the isomer. It is worth to notice also the work [31], analyzing decay of the ^{229m}Th via atomic Rydberg states.

Previously all the theorists [21–27] were discussing the EB, which only evolves discrete atomic spectra. A new step in this direction has been undertaken by Borisyuk *et al.* [32], who regarded the possibility to populate ^{229m}Th via the electron continuum. Indeed, this can be realized for the thorium atom, which has the ionization energy 6.3 eV, that is, the nuclear isomeric level is drowned in the electronic continuum spectrum. Such a fact facilitates laser tuning to the resonance. In the framework of quantum electrodynamics

*dzyublik@ukr.net

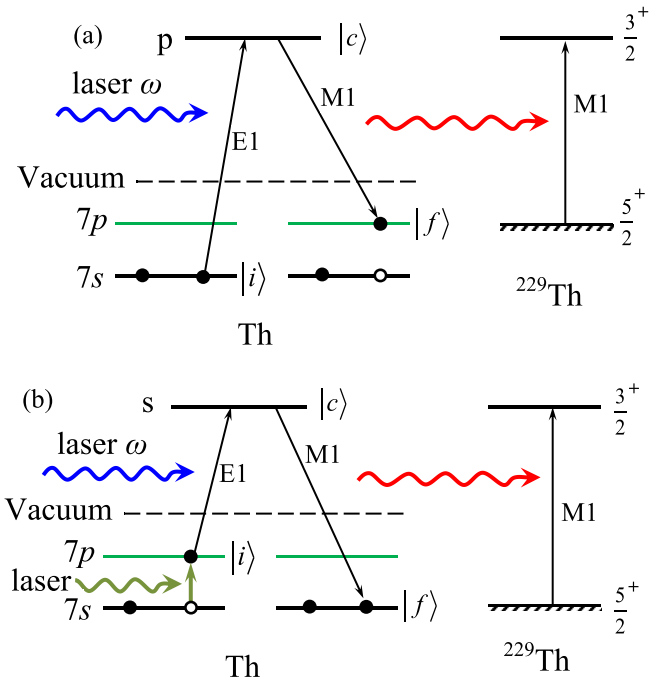

FIG. 1. Sketch of the EB via continuum, induced by laser, with excitation of the isomer ^{229m}Th. The continuum lies above the dashed line (vacuum). (a) EB begins from the upper $7s$ level of a Thorium atom and ends in the excited $7p$ one. (b) EB begins from the level $7p$, excited by the second laser, and ends when electron is captured by the atom into the $7s$ vacancy. In both cases ionization of the atom proceeds in $E1$ transitions. Resonant excitation of the nucleus happens at the reverse electron transitions of the same type and multipolarity as the nuclear $M1$ transition.

(QED) Borisyuk *et al.* [32] determined the EB cross section $\sigma_{\rm EB}$ of the isomer excitation and outlined possible schemes of the experiment. The authors considered three scenarios of EB, two of them are shown in the figure. In all three cases the atomic electron first absorbs the laser photon and flies away from the atom into the continuum spectrum. Then some of the electrons return into the atom, filling a vacancy and transferring its energy via virtual photons to the nucleus. The excited level ^{229m}Th afterwards decays through the radiative or conversion channel. In Ref. [32] it was shown that the contribution to photoionization cross section of the Th atom from $M1$ transitions is by eight orders weaker than from $E1$ transitions. Therefore in Fig. 1 only realistic EB are presented, which start with the electric dipole transitions.

The S matrix for such EB transition was calculated in Ref. [32] in the third order of the perturbation theory, introducing the complex energy $E_{\rm is} - i\Gamma_{\rm is}/2$ for the isomeric state, where $\Gamma_{\rm is}$ is the level width. This is typical procedure for the QED calculations of such kind. Then the wave function $\Psi_{\rm is}(x) = \Psi_{\rm is}(\mathbf{r})e^{-i(E_{\rm is}-i\Gamma_{\rm is}/2)}$ diverges as $t \to -\infty$. Therefore Borisyuk *et al.* integrated this function only at positive times t (see Eq. (4) of Ref. [32]), although in the chronologically ordered series for S_{fi} the integration over t is carried on the whole time axis [33]. By definition, the S matrix relates the initial and final states of the system, departed by the time interval $T \to \infty$. As is well known from the scattering theory [34–36], the transition probability per unit time and, respectively, the cross section are determined by the ratio $\lim_{T\to\infty}(|S_{fi}|^2/T)$. However, in Ref. [32] *ad hoc* the infinite time T was replaced by the isomer lifetime $\tau_{\rm is} = \hbar/\Gamma_{\rm is}$.

The main problem on the way of creation of the nuclear clock is an effective population of the ^{229m}Th and high-precision determination of its energy. This can be achieved only with lasers, having small frequency dispersion. Taking into account the great importance of this task, I rederive here the cross section for the EB through continuum, by applying strict methods of the scattering theory [34–36]. Possible realistic scenarios of EB, proposed in Ref. [32], are shown in Fig. 1. In case (a) the atomic electron from the upper $7s$ state absorbs the laser photon and performs $E1$ transition to the p state of the continuum, where it carries the orbital angular momentum $l = 1$. In the alternative case (b) the initial state is the $7p$ atomic level, excited by an additional laser, while in the intermediate s state $|c\rangle$, ensured again by $E1$ transition, $l = 0$. In both events the electron, coming back to the thorium atom, excites the isomer. The EB over the path $7s \to s \to 7s$ can be ignored, since the corresponding ionization cross section at $M1$ transition is by eight orders less than that at $E1$ transitions [32]. A similar EB process, generated in the K-electron capture by ^{153}Gd and leading to fusion of the energies of nuclear and atomic transitions, was considered in Ref. [37].

II. BASIS WAVE FUNCTIONS

The Hamiltonian of the whole system (^{229}Th + atomic electron + electromagnetic field) is written as

$$H = H_0 + V_r, \tag{1}$$

where the unperturbed Hamiltonian H_0 is represented by a sum of the Hamiltonians for the nucleus H_n, electron H_e and the field $H_{\rm rad}$, while the perturbation $V_r = V_r^n + V_r^e$ is responsible for interaction of the nucleus and electron with the field,

$$V_r^{n(e)} = -\frac{1}{c}\int \mathbf{J}_{n(e)}(\mathbf{r})\mathbf{A}(\mathbf{r})d\mathbf{r}, \tag{2}$$

where $\mathbf{J}_n(\mathbf{r})$ and $\mathbf{J}_e(\mathbf{r})$ are the electric current density operators for the nucleus and electron, respectively, $\mathbf{A}(\mathbf{r})$ is the vector potential operator of the field. The operator H_e is a sum of the kinetic energy operator of the electron and the screened Coulomb field of the nucleus $V_{\rm C}(r)$.

In the initial state of the system

$$|a\rangle = |I_g M_g\rangle\phi_{j_i m_i}(\mathbf{r})|1_{\mathbf{k}\lambda}\rangle \tag{3}$$

there are the nucleus in the ground state $|I_g M_g\rangle$ with spin I_g and its projection on the quantization axis M_g, the electron with the total angular momentum j_i and its projection m_i, and one photon with the wave vector $\mathbf{k}$ and circular polarization $\lambda = \pm 1$. The corresponding energy $E_a = \omega + \epsilon_i$, where ω is the energy of the incident photon (for brevity $\hbar$ is omitted), ϵ_i is the electron energy in the initial state $|j_i m_i\rangle$.

Having absorbed a photon, the electron passes to the continuous spectrum with the wave vector $\boldsymbol{\kappa}$, energy ε and spin

projection ν. Such a first intermediate state of the system is described by the wave function

$$|c_1\rangle = |I_g M_g\rangle \psi^+_{\boldsymbol{\kappa}\nu}(\mathbf{r})|0\rangle, \tag{4}$$

where $\psi^+_{\boldsymbol{\kappa}\nu}(\mathbf{r})$ describes the conversion electron, the factor $|0\rangle$ stands for the vacuum of the field.

Afterward the free electron can return to a vacant atomic level $|j_f m_f\rangle$ transferring its energy via a virtual photon to ^{229}Th, which goes to the excited isomeric level $|I_e M_e\rangle$ with spin and parity $I^\pi_e = 3/2^+$. The system then passes to the second intermediate state $|c_2\rangle$. The corresponding eigenvalues of H_0, associated with these intermediate states, are

$$E_{c_1} = \varepsilon, \qquad E_{c_2} = E_{\rm is} + \epsilon_f, \tag{5}$$

where ε means the energy of the conversion electron, ϵ_f is the final energy of the electron.

At the final stage of the EB process the isomer decays mainly through the conversion channel. In this case the final energy E_b equals the energy of the final conversion electron ε'.

Let us consider now in some details the distorted wave functions $\psi^+_{\boldsymbol{\kappa}\nu}(\mathbf{r})$, which describe scattering of electrons in the Coulomb field $V_{\rm C}(r)$. They are eigenfunctions of H_e with normalization

$$\int_0^\infty \psi^{+*}_{\boldsymbol{\kappa}\nu}(\mathbf{r})\psi^+_{\boldsymbol{\kappa}'\nu'}(\mathbf{r})d\mathbf{r} = \delta(\boldsymbol{\kappa}-\boldsymbol{\kappa}')\delta_{\nu\nu'}. \tag{6}$$

Forming a complete set, these functions are most suitable for description of the intermediate states of electrons in the continuous spectrum.

It is useful to expand $\psi^+_{\boldsymbol{\kappa}\nu}$ in partial waves [34]:

$$\psi^+_{\boldsymbol{\kappa}\nu}(\mathbf{r}) = \sum_{l=0}^\infty i^l e^{i\delta_l(\kappa)} \frac{w_l(\kappa;r)}{\kappa r} \sum_{m=-l}^{l} Y^*_{lm}(\hat{\boldsymbol{\kappa}}) Y_{lm}(\hat{\mathbf{r}}) u_{s\nu}, \tag{7}$$

where $u_{s\nu}$ is the spin factor ($s = 1/2,\ \nu = \pm 1/2$), the spherical angles of the vectors $\boldsymbol{\kappa}$ and $\mathbf{r}$ are denoted by $\hat{\boldsymbol{\kappa}}$ and $\hat{\mathbf{r}}$, respectively. The radial functions $w_l(\kappa;r)$ satisfy the equation

$$w_l''(\kappa;r) - [l(l+1)/r^2 + v(r) - \kappa^2] w_l(\kappa;r) = 0, \tag{8}$$

where the reduced potential

$$v(r) = 2\mu V_{\rm C}(r)/\hbar^2. \tag{9}$$

With growing r the screened Coulomb potential $V_{\rm C}(r)$ attenuates faster than a pure Coulomb one. Respectively, at $r \to \infty$ the functions $w_l(\kappa;r)$ have more simple asymptotics than the Coulomb functions [34]:

$$w_l(\kappa;r) \approx \sqrt{\frac{2}{\pi}} \sin\left(\kappa r - \frac{l\pi}{2} + \delta_l(\kappa)\right), \tag{10}$$

where $\delta_l(\kappa)$ stands for the phase shift.

Since the Hamiltonian H is invariant with respect to rotations it is more convenient to expand $\psi^+_{\boldsymbol{\kappa}\nu}(\mathbf{r})$ in terms of the eigenfunctions of the operators $\mathbf{j}^2$, $\mathbf{l}^2$, and j_z, where $\mathbf{j} = \mathbf{l} + \mathbf{s}$ is the total angular momentum operator of the electron, $\mathbf{l}$ and $\mathbf{s}$ are its orbital momentum and spin operators, respectively. Such eigenfunctions are represented by the generalized spherical harmonics [35]:

$$\mathscr{Y}^{m_c}_{j_c l s}(\hat{\mathbf{r}}) = \sum_{m\nu} (lsm\nu|j_c m_c) Y_{lm}(\hat{\mathbf{r}}) u_{s,\nu}, \tag{11}$$

where $(j_1 j_2 m_1 m_2|jm)$ are the Clebsh-Gordan coefficients. After substitution of the inverse transformation

$$Y_{lm}(\hat{\mathbf{r}}) u_{s\nu} = \sum_{j_c m_c} (lsm\nu|j_c m_c) \mathscr{Y}^{m_c}_{j_c l s}(\hat{\mathbf{r}}) \tag{12}$$

into the wave function (7), it takes the form

$$\psi^+_{\boldsymbol{\kappa}\nu}(\mathbf{r}) = \sum_{l=0}^\infty \sum_{j_c m_c} \phi_{j_c l m_c}(\mathbf{r}) \mathfrak{Y}^{m_c *}_{j_c}(lsv;\hat{\boldsymbol{\kappa}}), \tag{13}$$

depending on the products of the wave functions

$$\phi_{j_c l m_c}(\mathbf{r}) \equiv |j_c m_c\rangle = \frac{w_l(\kappa,r)}{\kappa r} \mathscr{Y}^{m_c}_{j_c l s}(\hat{\mathbf{r}}), \tag{14}$$

and subsidiary functions

$$\mathfrak{Y}^{m_c}_{j_c}(lsv;\hat{\boldsymbol{\kappa}}) = i^{-l} e^{-i\delta_l} \sum_{m=-l}^{l} (lsm\nu|j_c m_c) Y_{lm}(\hat{\boldsymbol{\kappa}}). \tag{15}$$

The functions $\phi_{j_c l m_c}(\mathbf{r})$ describe free electron, carrying the orbital momentum l and the total angular momentum j_c with projection m_c. They are normalized as

$$\int d\mathbf{r} \phi^*_{j_c l m_c}(\mathbf{r}) \cdot \phi_{j'_c l' m'_c}(\mathbf{r}) = \delta_{j_c j'_c} \delta_{l l'} \delta_{m_c m'_c}, \tag{16}$$

where the dot specifies a scalar product in the spin space.

From orthogonality relations for the Clebsh-Gordan coefficients as well as for spherical functions $Y_{lm}(\hat{\boldsymbol{\kappa}})$ it follows that

$$\sum_\nu \int d\Omega_{\boldsymbol{\kappa}} \mathfrak{Y}^{m'_c *}_{j'_c}(l'sv;\hat{\boldsymbol{\kappa}}) \mathfrak{Y}^{m_c}_{j_c}(lsv;\hat{\boldsymbol{\kappa}}) = \delta_{ll'}\delta_{j_c j'_c}\delta_{m_c m'_c}. \tag{17}$$

III. TRANSITION MATRIX

The EB transition $a \to b$ is determined by the T matrix,

$$T_{ba} = \sum_{c_2,c_1} \langle b|R|c_2\rangle G^+_{c_2 c_1}(E_a) \langle c_1|V_r|a\rangle, \tag{18}$$

where the level shift operator R is given by a series

$$R = V_r + V_r \frac{1}{E_a + i\eta - H_0} V_r + \ldots, \qquad \eta \to +0, \tag{19}$$

and $G^+_{c_2 c_1}(E_a)$ denotes the matrix of Green's operator

$$G^+(E_a) = (E_a + i\eta - H)^{-1}. \tag{20}$$

In (18) the summation over c_1 includes integration over the wave vector of the conversion electron $\boldsymbol{\kappa}$at infinity and summation over its spin projections $\nu = \pm 1/2$. The summation over c_2 is carried over the magnetic quantum numbers M_e and m_f.

In T_{ba} the factor $\langle b|R|c_2\rangle$ is associated with the decay of the isomeric $5/2^+$ level, whose total width is defined by standard

formula [34]:

$$\Gamma_{\rm is} = 2\pi \sum_b |\langle b|R|c_2\rangle|^2 \delta(E_b - E_a). \tag{21}$$

This $\Gamma_{\rm is}$ amounts the sum of the radiative partial width Γ_γ and the internal conversion width Γ_e.

Thus, there are two overlapping resonant levels $|c_1\rangle$ and $|c_2\rangle$, having the widths Γ_1 and Γ_2. Here $\Gamma_1/\hbar$ determines the rate of the electron capture from the continuous spectrum to any vacant atomic level, following by emission of a photon. In some cases the photon may be absorbed by the nucleus, exciting it. The latter effect, called nucleus excitation by electron capture (NEEC), was intensively explored in past years (see Ref. [38] and references therein). Γ_2 stands for the width $\Gamma_{\rm is}$ of the nuclear $3/2^+$ isomer. Notice also that the level $|c_2\rangle$ is degenerated over the magnetic quantum numbers. In this case the Green's matrix is determined by a system of algebraic equations [39]

$$\left(E_a - E_1 + i\frac{\Gamma_1}{2}\right) G^+_{c_1c_1} - \sum_{c_2} R^+_{c_1c_2} G^+_{c_2c_1} = 1,$$

$$-R^+_{c_2c_1} G^+_{c_1c_1} + \left(E_a - E_2 + i\frac{\Gamma_2}{2}\right) G^+_{c_2c_1} = 0, \tag{22}$$

where the R matrix

$$R^+_{c_1c_2} = \sum_{b' \neq c_1,c_2} \frac{V_{c_1b'} V_{b'c_2}}{E_a + i\eta - E_{b'}} + \ldots \tag{23}$$

is responsible for the NEEC process.

From Eqs. (22) it follows that the off-diagonal elements of Green's matrix are

$$G^+_{c_2c_1} = \frac{R^+_{c_2c_1}}{\left(E_a - E_1 + i\frac{\Gamma_1}{2}\right)\left(E_a - E_2 + i\frac{\Gamma_2}{2}\right) - \sum_{c_2} \left|R^+_{c_2c_1}\right|^2}. \tag{24}$$

The term $\sum_{c_2} |R_{c_2c_1}|^2$ may be eliminated here since it is much less than $\Gamma_{\rm is}\Gamma_1$. Substituting next (5) and (24) into (18) one can write the transition matrix in the form

$$T_{ba} = -\sum_{c_2,c_1} \frac{V'_{bc_2} R^+_{c_2c_1} V_{c_1a}}{(\varepsilon - \varepsilon_0 - i\Gamma_1/2)(\omega - \omega_{\rm res} + i\Gamma_{\rm is}/2)}, \tag{25}$$

where the energy $\varepsilon_0 = \hbar^2\kappa_0^2/2m_e = \omega + \epsilon_i$ indicates the maximum of the energy distribution of the virtual conversion electrons, $\omega_{\rm res} = E_{\rm is} + \epsilon_f - \epsilon_i$ is the resonance value of the laser photon energy.

The matrix element V_{c_1a} determines the first stage of the EB process, caused by absorption of the laser photon by an electron, which initially occupies the level $|j_im_i\rangle$. Applying the multipole expansion of the interaction V_r [40], one can write the matrix element for the $E1$ transition with absorption of one photon as

$$V_{c_1a} = -2\pi i\sqrt{\frac{2\hbar\omega}{3}} \times \sum_{\mu=-1}^{1} D^1_{\mu\lambda}(\alpha\beta 0) \langle \psi^+_{\boldsymbol{\kappa}\nu}|\mathfrak{N}_\mu(E1)\big|\phi_{j_im_i}\big\rangle, \tag{26}$$

where $D^1_{\mu\lambda}(\alpha\beta 0)$ is the rotation matrix, depending on the spherical angles β, α of the wave vector $\mathbf{k}$ of the photon with polarization $\lambda = \pm 1$. The electric dipole operator for the electron is given by

$$\mathfrak{N}_\mu(E1) = -erY_{1\mu}(\hat{\mathbf{r}}) \qquad (e > 0). \tag{27}$$

The R matrix, which determines exchange by virtual photon between two charged particles, has been calculated by Alder *et al.* (see Eq. (II B.15) in Ref. [41]). In accordance with their results, neglecting penetration of electrons inside the nucleus, one has for $M1$ transitions

$$R^+_{c_2c_1} = \frac{4\pi}{3} \sum_\mu (-1)^\mu \langle I_eM_e|\mathfrak{M}_\mu(M1)|I_gM_g\rangle \times \langle j_fm_f|\mathfrak{N}_{-\mu}(M1)|j_cm_c\rangle, \tag{28}$$

where $\mathfrak{M}_\mu(M1)$ and $\mathfrak{N}_\mu(M1)$ denote the magnetic dipole operators for the nucleus and electron, respectively. In the nonrelativistic approximation the magnetic dipole operator for the nucleus is [41]

$$\mathfrak{M}_\mu(M1) = \mu_n\sqrt{\frac{3}{4\pi}} \sum_{i=1}^{A} [g_l(i)l_\mu(i) + g_s(i)s_\mu(i)], \tag{29}$$

where $\mu_n = e\hbar/2m_pc$ is the nuclear magneton, m_p the mass of proton, $l_\mu(i)$ and $s_\mu(i)$ are the spherical projections of the orbital angular momentum and spin operators for the ith nucleon, $g_l(i)$, $g_s(i)$ the corresponding g factors.

At the same time, for the electron the magnetic dipole operator looks like [41]

$$\mathfrak{N}_\mu(M1) = -\frac{k^2}{2c} \int \mathbf{J}_e \cdot \mathbf{l}\big(h^{(1)}_1(kr)Y_{1\mu}(\hat{\mathbf{r}})\big) d\mathbf{r}, \tag{30}$$

where $h^{(1)}_l(x)$ is the spherical Hankel function of the first kind. In the same nonrelativistic (long-wave) approximation this reduces to

$$\mathfrak{N}_\mu(M1) = \mu_e\sqrt{\frac{3}{4\pi}}[l_\mu + 2s_\mu], \tag{31}$$

where $\mu_e = e\hbar/2m_ec$ is the Bohr magneton for the electron. However, only the exact operator (30) binds the states $|j_im_i\rangle$ and $|c\rangle$ but not its approximate version (31). Recall also that the spherical and Cartesian projections are connected by

$$j_0 = j_z, \quad j_{\pm 1} = \mp\frac{1}{\sqrt{2}}(j_x \pm j_y). \tag{32}$$

IV. CROSS SECTION

The cross section of the EB process is expressed by standard formula

$$\sigma_{\rm EB}(\omega) = \frac{2\pi}{\hbar c} \frac{1}{(2I_g + 1)(2j_i + 1)} \times \sum_{M_g,m_i} \sum_b |T_{ba}|^2 \delta(E_b - E_a). \tag{33}$$

Substituting here (25) and taking into account that the total width of the isomeric level is given by Eq. (21), one arrives at

$$\sigma_{\rm EB}(\omega) = (2\pi)^3 \frac{2k}{3}\left(\frac{4\pi}{3}\right)^2 \times \frac{\Gamma_{\rm is}}{(\omega-\omega_{\rm res})^2+(\Gamma_{\rm is}/2)^2}\mathcal{F}(\omega), \quad (34)$$

where the factor $\mathcal{F}(\omega)$ is

$$\mathcal{F}(\omega) = \frac{1}{(2I_g+1)(2j_i+1)}\sum_{M_e,M_g}\sum_{m_f,m_i}\left|\sum_{\mu\mu'}(-1)^{\mu+\mu'} \times \langle I_e M_e|\mathfrak{M}_\mu(M1)|I_g M_g\rangle D^1_{\mu'\lambda}(\alpha\beta 0)\mathcal{I}_{\mu\mu'}\right|^2, \quad (35)$$

and $\mathcal{I}_{\mu\mu'}$ designates the integral

$$\mathcal{I}_{\mu\mu'} = \int_0^\infty \frac{f_{\mu\mu'}(\kappa)\kappa^2 d\kappa}{\kappa^2-\kappa_0^2-i\gamma}, \qquad \gamma = m_e\Gamma_1/\hbar^2, \quad (36)$$

depending on the function

$$f_{\mu\mu'}(\kappa) = \frac{2m_e}{\hbar^2}\sum_\nu \int d\Omega_{\hat{\boldsymbol{\kappa}}}\langle j_f m_f|\mathfrak{N}_{-\mu}(M1)|\psi^+_{\boldsymbol{\kappa}\nu}\rangle \times \langle\psi^+_{\boldsymbol{\kappa}\nu}|\mathfrak{N}_{\mu'}(E1)|j_i m_i\rangle. \quad (37)$$

It simplifies by employing the expressions (13) for $\psi^+_{\boldsymbol{\kappa}\nu}$ and using the orthogonality relation (17):

$$f_{\mu\mu'}(\kappa) = \frac{2m_e}{\hbar^2}\sum_{j_c m_c}\langle j_f m_f|\mathfrak{N}_{-\mu}(M1)|j_c m_c\rangle \times \langle j_c m_c|\mathfrak{N}_{\mu'}(E1)|j_i m_i\rangle. \quad (38)$$

Further, the integral $\mathcal{I}_{\mu\mu'}$ is transformed to

$$\mathcal{I}_{\mu\mu'} = \frac{1}{2\kappa_0}\int_0^\infty f_{\mu\mu'}(\kappa) \times \left(\frac{1}{\kappa-\kappa_0-i\gamma'}-\frac{1}{\kappa+\kappa_0+i\gamma'}\right)\kappa^2 d\kappa. \quad (39)$$

Here $f_{\mu\mu'}(\kappa)$ is an even function, i.e., $f_{\mu\mu'}(-\kappa) = f_{\mu\mu'}(\kappa)$, since

$$w_l(-\kappa;r) = (-1)^l w_l(\kappa;r). \quad (40)$$

This allows us to rewrite the above integral as

$$\mathcal{I}_{\mu\mu'} = \frac{1}{2\kappa_0}\int_{-\infty}^\infty \frac{f_{\mu\mu'}(\kappa)\kappa^2 d\kappa}{\kappa-\kappa_0-i\gamma'} \quad (41)$$

with the integrand, which may be transformed to a product of smooth function and the sharp factor like a δ function

$$\frac{1}{\pi}\frac{\gamma'}{(\kappa-\kappa_0)^2+\gamma'^2} \approx \delta(\kappa-\kappa_0). \quad (42)$$

Therefore trivial estimation gives

$$\mathcal{I}_{\mu\mu'} = \pi i\rho(\varepsilon_0)\sum_{j_c m_c}\langle j_f m_f|\mathfrak{N}_{-\mu}(M1)|j_c m_c\rangle \times \langle j_c m_c|\mathfrak{N}_{\mu'}(E1)|j_i m_i\rangle, \quad (43)$$

where

$$\rho(\varepsilon_0) = \frac{\kappa m_e}{\hbar^2} \quad (44)$$

is the density of the electron states on the unit energy interval (see also Ref. [34]).

Next I use the fact that the transition matrix T_{ba} contains a number of matrix elements of the irreducible tensor operators $\mathfrak{M}_\mu(\lambda l)$ and $\mathfrak{N}_\mu(\lambda l)$, where $\lambda = E$ or M. Their dependence on the magnetic quantum numbers is determined by the Wigner-Eckart theorem (see, e.g., Ref. [42]). In particular,

$$\langle j_f m_f|\mathfrak{M}_\mu(\lambda l)|j_i m_i\rangle = \frac{(j_i l m_i\mu|j_f m_f)}{\sqrt{2j_f+1}}\langle j_f||\mathfrak{M}(\lambda l)||j_i\rangle, \quad (45)$$

where $\langle j_f||\mathfrak{M}(\lambda l)||j_i\rangle$ is the reduced matrix element, related to the reduced transition probability by [42]

$$B(\lambda l; i\to f) = (2j_i+1)^{-1}|\langle j_f||\mathfrak{M}(\lambda l)||j_i\rangle|^2. \quad (46)$$

Keeping also in mind the orthogonality rule for the Clebsh-Gordan coefficients

$$\sum_{m_1 m}(j_1 j_2 m_1 m_2|jm)(j_1 j_2' m_1 m_2'|jm) = \frac{2j+1}{2j_2+1}\delta_{j_2 j_2'}\delta_{m_2 m_2'}, \quad (47)$$

unitarity of the Wigner functions

$$\sum_{\mu=-j}^{j} D^{j*}_{\mu\nu}(\alpha\beta\gamma)D^j_{\mu\nu'}(\alpha\beta\gamma) = \delta_{\nu\nu'}, \quad (48)$$

as well as the connection of the reduced probabilities for direct and reverse transitions

$$\frac{B(\lambda l; i\to f)}{B(\lambda l; f\to i)} = \frac{2j_f+1}{2j_i+1}, \quad (49)$$

one arrives at

$$\mathcal{F}(\omega) = \rho^2(\varepsilon_0)\left(\frac{\pi}{3}\right)^2 g_{j_c}B_n(M1; I_e\to I_g) \times \sum_{j_c} B_e(M1; j_f\to j_c)B_e(E1; j_i\to j_c), \quad (50)$$

where the reduced probabilities B_n and B_e refer to the nuclear and electronic transitions, respectively, and the spin factor

$$g_{j_c} = \frac{2I_e+1}{2I_g+1}\frac{2j_f+1}{2j_c+1}. \quad (51)$$

For the EB, shown in Fig. 1(a), the intermediate electron state $|c\rangle$ is a coherent mixture of the waves with angular momenta $j_c = 1/2$ and $j_c = 3/2$, while for the EB in Fig. 1(b) it reduces to single wave with $j_c = 1/2$.

Substitution of (50) into (34) completely determines the EB cross section:

$$\sigma_{\rm EB}(\omega) = \sum_{j_c}\sigma^{j_c}_{\rm EB}(\omega), \quad (52)$$

where the partial cross section for the branching transition via the electron state j_c with the positive energy ε is

$$\sigma^{j_c}_{\rm EB}(\omega) = \frac{1}{8}g_{j_c}\frac{\Gamma_{\rm is}\Gamma^{j_c}_{\rm IC}(f)}{(\omega-\omega_{\rm res})^2+(\Gamma_{\rm is}/2)^2}\sigma^{j_c}_{\rm ion}(\omega). \quad (53)$$

Besides, here $\sigma_{\rm ion}^{j_c}(\omega)$ is the partial ionization cross section for an atomic electron, occupying initially the j_i shell and carrying away the total angular momentum j_c:

$$\sigma_{\rm ion}^{j_c}(\omega) = (2\pi)^4 \frac{4k}{9} B_e(E1; j_i \to j_c)\rho(\varepsilon_0), \tag{54}$$

while the complete ionization cross section is

$$\sigma_{\rm ion}(\omega) = \sum_{j_c} \sigma_{\rm ion}^{j_c}(\omega). \tag{55}$$

The partial width for the internal electron conversion through transition $j_f \to j_c$ is given by

$$\Gamma_{\rm IC}^{j_c}(f) = 4\left(\frac{2\pi}{3}\right)^3 B_n(M1; I_e \to I_g) \times B_e(M1; j_f \to j_c)\rho(\varepsilon_0) \tag{56}$$

and complete width $\Gamma_{\rm IC}$ is a sum of $\Gamma_{\rm IC}^{j_c}$.

For the transition $(a) = \{s \to p \to p\}$, shown in Fig. 1(a), the intermediate electron state $|c\rangle$ is a coherent mixture of the waves with angular momenta $j_c = 1/2$ and $j_c = 3/2$. On the electron path $(b) = \{p \to s \to s\}$, shown in Fig. 1(b), it reduces to single wave with $j_c = 1/2$. By employing Eqs. (11) and (13) for the wave functions $|j_c m_c\rangle$, one finds that in the first case

$$B_e(E1; 1/2 \to 3/2) = 2B_e(E1; 1/2 \to 1/2). \tag{57}$$

Respectively, the partial ionization cross sections are

$$\sigma_{\rm ion}^{3/2}(\omega) = \tfrac{2}{3}\sigma_{\rm ion}(\omega), \qquad \sigma_{\rm ion}^{1/2}(\omega) = \tfrac{1}{3}\sigma_{\rm ion}(\omega). \tag{58}$$

Then, combining (33), (53), and (58), one can rewrite the EB cross section for the transition [Fig. 1(a)] as

$$\sigma_{\rm EB}^{(a)}(\omega) = \frac{1}{24}\frac{\Gamma_{\rm is}\left(2g_{3/2}\Gamma_{\rm IC}^{3/2} + g_{1/2}\Gamma_{\rm IC}^{1/2}\right)}{(\omega-\omega_{\rm res})^2 + (\Gamma_{\rm is}/2)^2}\sigma_{\rm ion}(\omega). \tag{59}$$

If the laser frequency is tuned to resonance, i.e., $\omega = \omega_{\rm res}$, then ε_0 coincides with the energy $\varepsilon_0 = E_{\rm is} - |\epsilon_f|$ of the ejected electron in standard IC experiment without any lasers.

The radiation emitted by a laser source is characterized by some energy distribution $w_s(\omega)$, concentrated at the energy ω_0, having the width Γ_s and normalized to unity:

$$\int_0^\infty w_s(\omega)d\omega = 1. \tag{60}$$

In order to find the experimentally measured cross section we should average $\sigma_{\rm ion}^{j_c}(\omega)$ over $w_s(\omega)$:

$$\left\langle\sigma_{\rm ion}^{j_c}(\delta)\right\rangle = \int_{-\infty}^{\infty} d\omega w_s(\omega)\sigma_{\rm ion}^{j_c}(\omega), \tag{61}$$

where δ is a detuning of the incident laser pulse from the resonance,

$$\delta = \omega_{\rm res} - \omega_0. \tag{62}$$

Following Ref. [32] I take the Lorentzian distribution

$$w_s(\omega) = \frac{1}{2\pi}\frac{\Gamma_e}{(\omega-\omega_0)^2 + (\Gamma_s/2)^2}. \tag{63}$$

Inserting into (61) its integral representation

$$w_s(\omega) = \frac{1}{\pi}{\rm Re}\int_0^\infty d\mu e^{i(\omega-\omega_0)\mu - \Gamma_s\mu/2} \tag{64}$$

and applying the contour integration one finds

$$\left\langle\sigma_{\rm EB}^{j_c}(\delta)\right\rangle = \left\langle\sigma_{\rm EB}^{j_c}(0)\right\rangle\frac{(\Gamma/2)^2}{\delta^2 + (\Gamma/2)^2}, \tag{65}$$

where $\Gamma = \Gamma_s + \Gamma_{\rm is}$ and the resonant value of the averaged cross section is

$$\left\langle\sigma_{\rm EB}^{j_c}(0)\right\rangle = \frac{1}{2}g_{j_c}\frac{\Gamma_{\rm IC}^{j_c}}{\Gamma}\sigma_{\rm ion}^{j_c}(\omega_{\rm res}). \tag{66}$$

The isomer ^{229m}Th mainly decays through the internal conversion channel ($\alpha \approx 10^9$), so that $\Gamma_{\rm IC}(7s) \approx \Gamma_{\rm is}$. Therefore the resonant value of the cross section, corresponding to the path [Fig. 1(b)], will be

$$\langle\sigma_{\rm EB}(0)\rangle_b \approx \frac{1}{2}\left(\frac{2I_e+1}{2I_g+1}\right)\frac{\Gamma_{\rm is}}{\Gamma_s+\Gamma_{\rm is}}\sigma_{\rm ion}(\omega_{\rm res}). \tag{67}$$

Let us compare it with the absorption cross section of ultraviolet photons, averaged over the same distribution (63),

$$\langle\sigma_\gamma(\delta)\rangle = \langle\sigma_\gamma(0)\rangle\frac{(\Gamma/2)^2}{\delta^2 + (\Gamma/2)^2}, \tag{68}$$

with the cross section at the resonance

$$\langle\sigma_\gamma(0)\rangle = \frac{2\pi}{k_0^2}\left(\frac{2I_e+1}{2I_g+1}\right)\frac{\Gamma_{\rm is}^\gamma}{\Gamma}, \tag{69}$$

where $k_0 = \omega_0/c$ and $\Gamma_{\rm is}^\gamma$ is the partial radiation width of the isomer [$\Gamma_{\rm is}^\gamma = \Gamma_{\rm is}/(1+\alpha) \approx 10^{-9}\Gamma_{\rm is}$]. Taking the value $\sigma_{\rm ion}(8.3\ {\rm eV}) \approx 3 \times 10^{-18}\ {\rm cm}^2$, calculated in Ref. [32], one gets the estimation $\langle\sigma_\gamma(0)\rangle/\langle\sigma_{\rm IB}(0)\rangle_b \approx 0.02$. In the case (a) the cross section $\langle\sigma_{\rm EB}^{(a)}(0)\rangle$ is by order of magnitude less than $\langle\sigma_{\rm EB}(0)\rangle_b$ (see also Ref. [32]).

V. CONCLUSION

I derived Eqs. (33), (53) for the cross section of the electron bridge via continuum, generated by a monochromatic laser wave, as well as Eqs. (65)–(67) for the EB cross section, averaged over the frequency distribution of incident photons (63). It is shown that the T matrix, which describes transition $(a) = 7s \to p \to 7p$, splits into two terms, corresponding to the intermediate electron states in the continuum with the angular momenta $j_c = 1/2$ and $3/2$. Straightforward calculations show that such amplitudes do not interfere, but give rise to the EB cross section $\sigma_{\rm EB}(\omega)$ as a sum of two terms with $j_c = 1/2$ and $3/2$. Besides, Eq. (53) for the spin factor g does not contain a spurious factor $(2j_c+1)^{-2}$, taking place in [32], but Eq. (53) contains extra factor $1/8$.

As a whole, my calculations confirm the conclusion of the paper [32] that EB via continuum, and especially its version (b), is more perspective than the direct photoexcitation of the isomer ^{229m}Th. The EB via the continuum has also an advantage compared to the EB via discrete atomic levels (see also Ref. [32]). In the last case we have to realize two resonances. At first, the laser frequency ω should match the

transition frequency in the atom ω_a, i.e., it should be $\omega \approx \omega_a = (\epsilon_c - \epsilon_i)/\hbar$, where ϵ_i, ϵ_c and ϵ_f are the energies of initial, intermediate and final atomic levels. Furthermore, we have to provide one more constraint $\omega \approx (E_{\rm is} + \epsilon_f - \epsilon_i)/\hbar$. Comparing these two requirements we get the main resonance condition for the atomic and nuclear transitions $E_{\rm is} \approx \epsilon_c - \epsilon_f$, which ensures effective transfer of the atomic energy to the nucleus. Note that the same resonance condition is needed for nuclear excitation by electron transition (NEET), theoretically studied in Refs. [42–49]. However, it is difficult to find such atomic transitions between bound levels, which are almost in the resonance with the nuclear transition. At the same time, in the case of the continuum EB two resonance conditions, which are reduced to single one $\omega \approx \omega_{\rm res}$, are always fulfilled automatically.

As an additional advantage of the scheme (b) Borisyuk *et al.* [32] indicated that the photons emitted in the atomic transition from the $7p$ level to $7s$ one may serve as a signal of the isomer excitation. But their detection only indicates that the $7p$ level is populated under the influence of the first laser. At the same time, as a benchmark of the population of ^{229m}Th one can employ the products of its decay: the conversion electrons. The prompt photoelectrons are emitted during the action of the laser pulse, while the delayed conversion electrons are ejected during the isomer decay. These electrons are easily separated in the time-delay experiment by choosing duration of the laser pulse $\tau_s = \hbar/\Gamma_s$ much larger than the isomer lifetime $\tau_{\rm is} = \hbar/\Gamma_{\rm is}$. However, this corresponds to wide frequency distribution of the laser photons, $\Gamma_s \gg \Gamma_{\rm is}$ and, respectively, to weakening of the counting rate of successful events.

Typical experiments with the optical clock are performed with ions in a neutral gas, captured in the Paul trap [50]. There the electric field, oscillating with the frequency Ω, hold the ions in a confined volume. The spectra of such ions consist of the central line and the side bands spaced by Ω. The EB cross section in the case of ions conserves the same form (33), (53). Nevertheless, the ionization cross section $\sigma_{\rm ion}^{3/2}(\omega)$ and the width $\Gamma_{\rm IC}^{j_c}(f)$ depend on the number of outer electrons involved in the process. In particular, in the scheme (a) $\sigma_{\rm ion}^{3/2}(\omega)$ for Th^+ is half a cross section for the neutral atom. Peculiarities of the most realistic two-laser experiment (b) will be analyzed in the next paper.

ACKNOWLEDGMENTS

I thank Prof. E. V. Tkalya for fruitful discussion and Dr. P. V. Borisyuk for helpful remarks. The research was supported by a grant of the Russian Science Foundation (Project No. 19-72-30014).

[1] E. Peck and C. Tamm, Europhys. Lett. **61**, 181 (2000).
[2] W. G. Rellergert, D. DeMille, R. R. Greco, M. P. Hehlen, J. R. Torgerson, and E. R. Hudson, Phys. Rev. Lett. **104**, 200802 (2010).
[3] C. J. Campbell, A. G. Radnaev, A. Kuzmich, V. A. Dzuba, V. V. Flambaum, and A. Derevianko, Phys. Rev. Lett. **108**, 120802 (2012).
[4] E. V. Tkalya, Phys. Rev. Lett. **106**, 162501 (2011).
[5] V. V. Flambaum, Phys. Rev. Lett. **97**, 092502 (2006).
[6] H.-T. He and Z.-Z. Ren, J. Phys. G: Nucl. Phys. **34**, 1611 (2007).
[7] A. Hayes and J. Friar, Phys. Lett. B **650**, 229 (2007).
[8] E. Litvinova, H. Feldmeier, J. Dobaczewski, and V. Flambaum, Phys. Rev. C **79**, 064303 (2009).
[9] J. C. Berengut, V. A. Dzuba, V. V. Flambaum, and S. G. Porsev, Phys. Rev. Lett. **102**, 210801 (2009).
[10] E. V. Tkalya *et al.*, Phys. Scr. **53**, 296 (1996).
[11] L. Kroger and C. Reich, Nucl. Phys. A **259**, 29 (1976).
[12] R. G. Helmer and C. W. Reich, Phys. Rev. C **49**, 1845 (1994).
[13] Z. O. Guimaräes-Filho and O. Helene, Phys. Rev. C **71**, 044303 (2005).
[14] B. R. Beck, J. A. Becker, P. Beiersdorfer, G. V. Brown, K. J. Moody, J. B. Wilhelmy, F. S. Porter, C. A. Kilbourne, and R. L. Kelley, Phys. Rev. Lett. **98**, 142501 (2007).
[15] A. Yamaguchi, H. Muramatsu, T. Hayashi, N. Yuasa, K. Nakamura, M. Takimoto, H. Haba, K. Konashi, M. Watanabe, H. Kikunaga, K. Maehata, N. Y. Yamasaki, and K. Mitsuda, Phys. Rev. Lett. **123**, 222501 (2019).
[16] L. von der Wense, B. Seiferle, M. Laatiaoui, J. B. Neumayr, H.-J. Maier, H.-F. Wirth, C. Mokry, J. Runke, K. Eberhardt, C. E. Düllmann, N. G. Trautmann, and P. G. Thirolf, Nature (London) **533**, 47 (2016).
[17] B. Seiferle, L. von der Wense, P. V. Bilous, I. Amersdorffer, C. Lemell, F. Libisch, S. Stellmer T. Schumm, C. E. Düllmann, A. Pálffy, and P. G. Thirolf, Nature (London) **573**, 243 (2019).
[18] M. Verlinde *et al.*, Phys. Rev. C **100**, 024315 (2019).
[19] J. Jeet, C. Schneider, S. T. Sullivan, W. G. Rellergert, S. Mirzadeh, A. Cassanho, H. P. Jenssen, E. V. Tkalya, and E. R. Hudson, Phys. Rev. Lett. **114**, 253001 (2015).
[20] T. Masuda *et al.*, Nature (London) **573**, 238 (2019).
[21] E. V. Tkalya, JETP Lett. **55**, 216 (1992).
[22] E. V. Tkalya, Sov. J. Nucl. Phys. **55**, 1611 (1992).
[23] P. Kalman and T. Keszthelyi, Phys. Rev. C **49**, 324 (1994).
[24] F. F. Karpeshin, I. M. Band, and M. B. Trzhaskovskaya, Nucl. Phys. A **654**, 579 (1999).
[25] S. G. Porsev, V. V. Flambaum, E. Peik, and C. Tamm, Phys. Rev. Lett. **105**, 182501 (2010).
[26] S. G. Porsev and V. V. Flambaum, Phys. Rev. A **81**, 042516 (2010).
[27] F. F. Karpeshin and M. B. Trzhaskovskaya, Phys. Rev. C **95**, 034310 (2017).
[28] V. A. Krutov and V. N. Fomenko, Ann. Phys. (NY) **476**, 291 (1968).
[29] L. von der Wense, B. Seiferle, S. Stellmer, J. Weitenberg, G. Kazakov, A. Pálffy, and P. G. Thirolf, Phys. Rev. Lett. **119**, 132503 (2017).
[30] J. Thielking, M. Okhapkin, P. Glowacki, D. M. Meier, L. von der Wense, B. Seiferle, P. G. Thirolf, E. Peik, and C. E. Düllmann, Nature (London) **556**, 321 (2018).
[31] E. V. Tkalya, Phys. Rev. C **100**, 054316 (2019).
[32] P. V. Borisyuk, N. N. Kolachevsky, A. V. Taichenachev, E. V. Tkalya, I. Yu. Tolstikhina, and V. I. Yudin, Phys. Rev. C **100**, 044306 (2019).

[33] V. B. Berestetskii, E. M. Lifschitz, and L. P. Pitaevskii, *Quantum Electrodynamics* (Pergamon, Oxford, 1982).
[34] M. L. Goldberger and K. M. Watson, *Collision Theory* (J. Wiley, New York, 1967).
[35] R. G. Newton, *Scattering Theory of Waves and Particles* (Springer, New York, 1982).
[36] A. G. Sitenko, *Lectures in Scattering Theory* (Springer, Berlin, 1991).
[37] A. Ya. Dzyublik, Phys. Atom. Nucl. **79**, 351 (2016).
[38] Y. Wu, C. H. Keitel, and A. Pálffy, Phys. Rev. Lett. **122**, 212501 (2019).
[39] A. Ya. Dzyublik, Sov. J. Theor. Math. Phys. **87**, 393 (1991).
[40] A. S. Davydov, *Theory of Atomic Nucleus* (Fizmatgiz, Moscow, 1958) (in Russian).
[41] K. Alder, A. Bohr, T. Huus, B. Mottelson, and A. Winther, Rev. Mod. Phys. **28**, 432 (1956).
[42] A. S. Davydov, *Excited States of Atomic Nuclei* (Atomizdat, Moscow, 1966) (in Russian).
[43] M. Motita, Prog. Theor. Phys. **49**, 1574 (1973).
[44] E. V. Tkalya, Nucl. Phys. A **539**, 209 (1992).
[45] M. R. Harston, Nucl. Phys. A **690**, 447 (2001).
[46] E. V. Tkalya, Phys. Rev. C **68**, 064611 (2003).
[47] E. V. Tkalya, Phys. Rev. A **75**, 022509 (2007).
[48] A. Ya. Dzyublik, JETP Lett. **93**, 489 (2011).
[49] A. Ya. Dzyublik, Phys. Rev. C **88**, 054616 (2013).
[50] A. D. Ludlow, M. M. Boyd, J. Ye, E. Peik, and P. O. Schmidt, Rev. Mod. Phys. **87**, 637 (2015).